A Shuttlecock Optical Rotator—Its Design, Fabrication and Evaluation for a Microfluidic Mixer

Hiroo Ukita and Motoki Kanehira

***Abstract*—An optically driven microrotator is proposed for fluidic mixing in future micrototal analysis systems (μ-TAS). The rotation mechanism, optical torque and microflow around the rotator are analyzed, and the rotator is fabricatied both by photolithography and photoforming methods. The microflow fields generated by the optical rotation are then experimentally visualized by both tracer and optical methods, and the velocity vectors and flux amount around the rotator are analyzed for the evaluation of the mixing performance of the microfluids.**

***Index Terms*—μ-TAS, fluidic mixing, flux amount, microflow, micrototal analysis systems, optical rotator, optical torque, optical tweezers, photoforming, photolithography, shuttlecock rotator, tracer, velocity vector, visualization.**

I. Introduction

OPTICAL tweezers have been successfully utilized in various scientific and engineering fields such as biology, microchemistry, physics, optics, and micromechanics [1]. The ability to rotate microobjects offers important applications in optical MEMS and biotechnology. This article describes an optical rotator design, fabrication, and evaluation to increase the mixing performance of microliquids for future fluidic applications such as micrototal analysis systems (μ-TAS) [2]. The rotator will be used as a mixer in a labs-on-a-chip shown in Fig. 1. The chip will have components such as inlets for the sample and reagent loading, microfabricated fluidic channels with a mixing chamber and an analyzing chamber, a detector for the reaction products, and outlets for sample waste. The analyte specimen and the reagents will be actuated by pressure force using syringe pumps.

Due to the small Reynolds number, micromixing devices are fabricated to increase the contact area to promote the diffusion effect by interweaving the two fluids. This interweaving has been done by structure geometry in a channel such as micronozzle arrays [3] and intersecting channels [4] which induce chaotic behavior [5] of a flow. These mixers have been characterized as static devices. On the other hand, an active silicon micromixer with a thin piezoelectrically actuated membrane [6] to generate a strong lateral acoustic thrust in a liquid has been presented. We now propose another type of active method to stir a liquid by an optically driven microrotator.

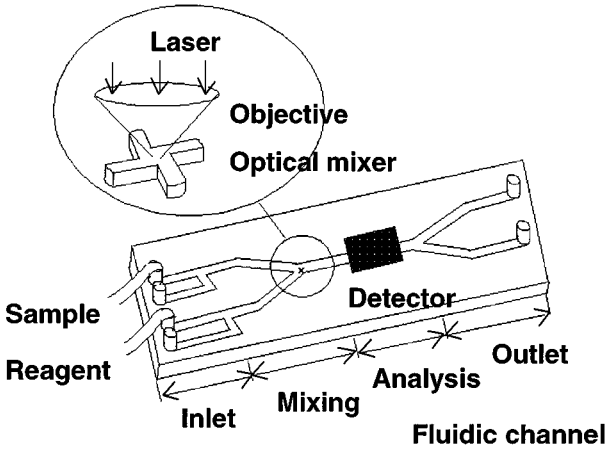

Fig. 1. Concept of an optical mixer which will be used in future labs-on-a-chip. The chip will have components such as inlets, fluidic channels with a mixing chamber, a detector and outlets.

In the design, three-dimensional (3-D) rotator shapes are analyzed based on the optical torque using a ray optics model and the flow field around the rotator is analyzed using computational fluid dynamics (CFD) by the finite volume method. For the fabrication, two methods are employed; conventional photolithography [7] and microphotoforming [8]. A new apparatus employing a spinner is developed to form a very thin laminated layer for the latter method [9]. Shuttlecock rotators of 30 μm in diameter are made from visible light-curable resin using an optical head for a DVD.

In the evaluation, the microflow fields generated by the optical rotator are analyzed through visualized images obtained using a newly constructed evaluation system [10]. For the visualization, we use two improved methods. One is the tracer method in which we trace many particles suspended in the medium. The other is an optical method in which we observe medium density variation [11]. By comparing the two methods, we confirmed that the optical method is appropriate to visualize the total liquid flow behavior.

We analyzed the microliquid velocity vectors and flux amount around the rotators as an index of the agitation. Through the analysis, we confirmed both the rotator shape and the rotation velocity affect on the microliquid flow and that the fluid motion expands to twice or three times the rotator diameter even on a microscale.

Manuscript received July 9, 2001; revised December 13, 2001. This work was supported in part by the Proposed Based New Industry Creative Type Technology Research and Development Promotion Program from the New Energy and Industrial Technology Development Organization (NEDO) of Japan.

The authors are with the Faculty of Science and Engineering, Ritsumeikan University, 525-8577 Shiga, Japan.

Publisher Item Identifier S 1077-260X(02)02225-6.

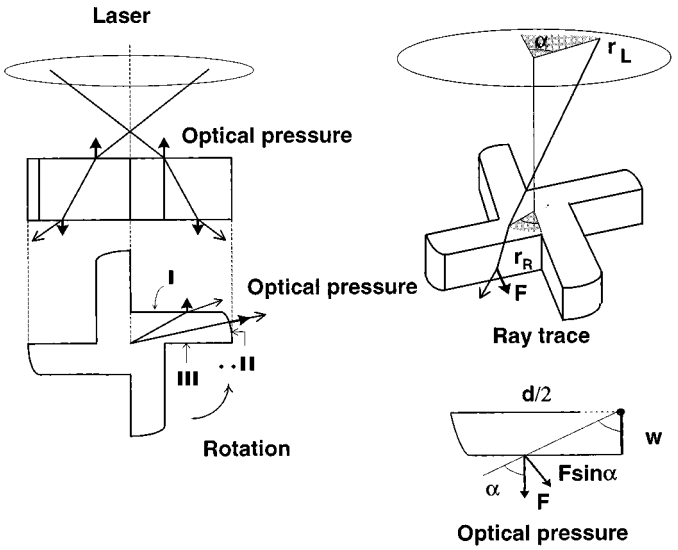

Fig. 2. Fundamental shapes of a shuttlecock optical rotator and rotation principle by the optical pressure induced on side surface I.

II. Design of the Shuttlecock Optical Rotator

A. Optical Torque

Fig. 2 shows the optical rotation principle of a shuttlecock type rotator which has no bilateral symmetry in the horizontal cross section [12], [13]. In the left figure, when the incident laser light is refracted at the top surface, the momentum changes and an upward optical pressure force is exerted, which leads to lifting the rotator. An optical pressure force is also exerted when the laser light is emitted from the side surfaces. We considered the three side surfaces I, II, and III of one particular wing. The optical pressure force is exerted on the side surfaces I and II, but not on side surface III, because surface III is parallel to the radial direction and does not refract the light. When the light is emitted from side surface II, it does not contribute to the torque because its direction is radial. Therefore, the torque, which rotates the rotator counterclockwise comes from only the optical pressure force on side surface I.

The right figure shows the ray tracing to simulate the torque for the rotator illuminated with a focused beam. We traced the rays until they hit the bottom surface. The beam was divided into about 2500 equal area segments on the aperture. We considered a ray incidence (r_L, α) on the lens and estimated the torque at the point r_R on side surface I. The radius r_R is expressed as

$$r_R = \frac{w}{\cos\,\alpha} \tag{1}$$

where w is the wing width. The optical torque T at r_R is,

$$T = r_R F\,\sin\,\alpha. \tag{2}$$

The total optical torque M exerted on the four wing surfaces is

$$M = 4\int_{\alpha=0}^{\alpha=\cos^{-1}(2w/d)} \int_{r_{L\min}}^{r_{L\max}} Fr^2\,dr\,d\alpha \tag{3}$$

where d is the shuttlecock diameter, and $r_{L\min}$ and $r_{L\max}$ are the minimum and maximum distances from the optical axis, respectively. They are given as $r_{L\min} = 0$ and

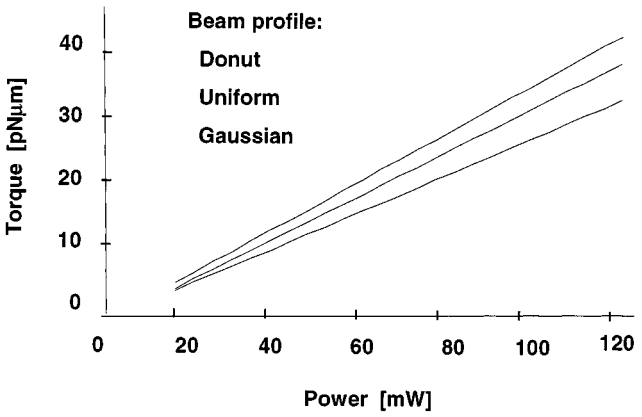

Fig. 3. Simulated optical torque dependence on laser power for a shuttlecock rotator for donut, uniform and Gaussian beam profiles.

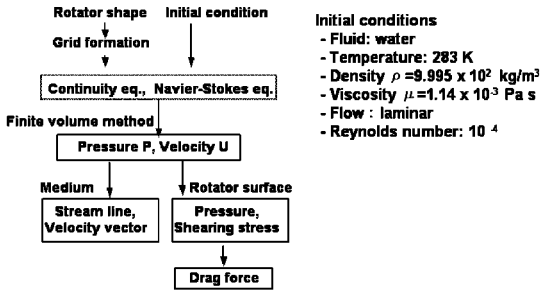

Fig. 4. Process of the flow field and drag force analysis with a computational fluid dynamics.

$r_{L\max} = \tan\{\arcsin(NA/n_1)\}$, where NA and n_1 are the objective lens numerical aperture and surrounding medium refractive index, respectively.

Fig. 3 shows the simulated result for the rotator height $h = 5.0$ μm, the diameter $d = 15$ μm, the wing width $w = 2.5$ μm, and beam profiles as parameters, where the refractive index $n_2 = 1.5$ and $n_1 = 1.33$. The optical torque is linearly proportional to the input power and a high torque can be obtained by a donut beam profile, since it has a strong intensity at the outer part of the aperture [14]. The rotation speed is determined by balancing the optical torque with the drag force of the rotator. Furthermore, the speed becomes high as the NA increases, because the large divergence angle increases the amount of light emitted from the side.

B. Microflow Around the Rotator

To evaluate the performance of the liquid mixing in microscale systems, the microflow around the rotator was investigated as shown in Fig. 4 using a fluid flow solver [15].

The simulation was performed in a 3-D geometry with a commercial computational fluid dynamics tool (CFX-4, AEA Corp.). The control volume is a cube, each domain has a set of discretized equations that are formulated by evaluating and integrating the fluxes across the faces of the volume to satisfy the conservation (4) and (5), where $\mathbf{U}$ is the fluid velocity $\mathbf{u}$ is the velocity of the sliding mesh, t is the time, P is the pressure, and ν is the kinematic viscosity [16].

$$\nabla \bullet (\mathbf{U} - \mathbf{u}) = 0 \tag{4}$$

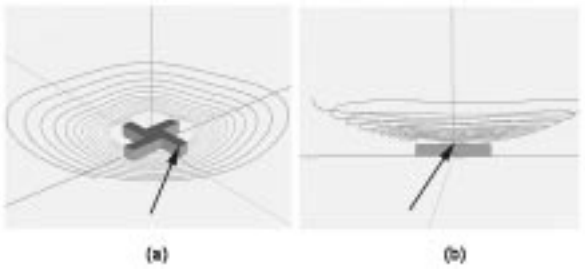

Fig. 5. Stream lines around the rotator after two seconds at a speed of 50 rpm. (a) Squint view. (b) side view.

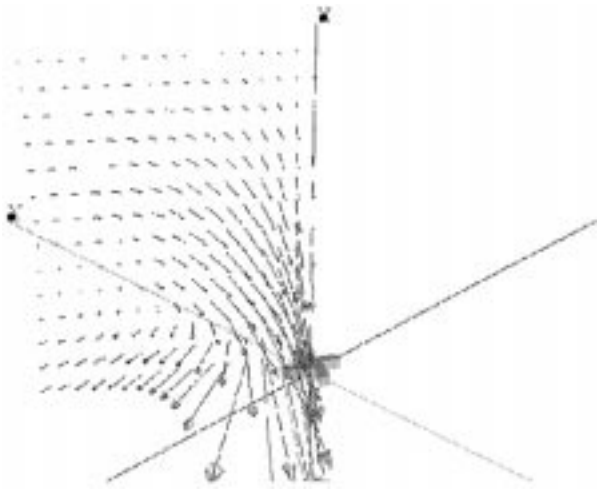

Fig. 6. Velocity vectors in the proximity of the rotator after two seconds at the speed of 50 rpm.

$$\frac{\partial \mathbf{U}}{\partial t} + ((\mathbf{U} - \mathbf{u}) \bullet \nabla)\mathbf{U} = -\nabla P + \nu \nabla^2 \mathbf{U}. \qquad (5)$$

To discretize (4) and (5), the finite volume method is used. The solver runs through a number of iterations trying to minimize the overall change in selected parameters from one iteration to another. We obtained the pressure P and velocity $\mathbf{U}$ for each volume.

The stream lines (Fig. 5) and the velocity vectors (Fig. 6) in the proximity of the rotator after 2 s at the speed of 50 rpm were analyzed for the same rotator described above. The Reynolds number ($Re = r\omega d^2/4\pi$) equals 10^{-4}. From both figures, we confirmed that the velocity increases close to the rotator and the flow goes both outward and upward, which promote fluid mixing.

III. Fabrication of the Shuttlecock Optical Rotator

Besides the specially fabricated rotator, the controlled rotation of trapped particles in an interference pattern between a Laguerre–Gaussian beam and a plane wave was recently reported [17], but it will not be widely applicable because of its complicated set up. We fabricated shuttlecock optical rotators by both photolithography and microphotoforming. Fig. 7 shows the two-dimansional (2-D) photoresist rotators with 30-, 20-, and 10-μm diameters fabricated by conventional photolithography [6]. We released the rotator into the laser trap environment by etching the aluminum under the resist.

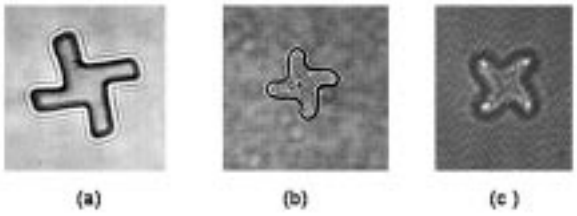

Fig. 7. Shuttlecock optical rotators of (a) 30 μm, (b) 20 μm, and (c) 10 μm in diameter fabricated by photolithography.

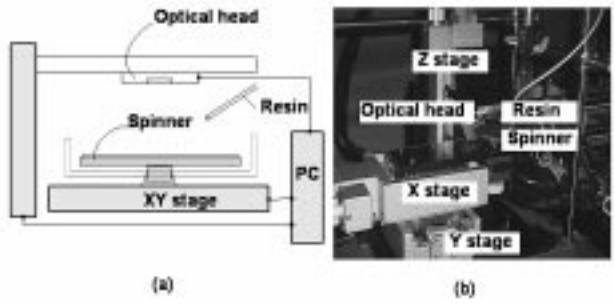

Fig. 8. (a) Schematic diagram. (b) Photograph of the spinner type microphotoforming apparatus.

In order to promote the optical torque, the rotator should have a 3-D structure with slopes on its upper surface [14]. The photoforming method can be used to fabricate 3-D microstructures. Nevertheless, the already proposed microphotoforming apparatus is large and requires a special laser beam (ultrashort-pulsed near-infrared Ti : sapphire) or special resin (two-photon-absorbed urethane material) [18].

We have developed a desk top microphotoforming apparatus using a DVD optical head and a visible light-curable resin (DF-200N, Nippon Kayaku Corp.), both commercially available. Since the microstructure is obtained by scanning a focused laser beam to solidify the contour of a liquid photopolymer, the resolution is determined by the laser beam intensity distribution and the absorption of light within the polymer. To decrease the solidified depth, a thin resin film was made by a spinner as shown in Fig. 8.

Fig. 9 shows the shuttlecock optical rotator with a 30 μm diameter and 15 μm thickness. The fabrication conditions were a scan speed of 25 μm/s, scan pitch of 1 μm, single scan and a laser power of 0.35 mW. The overall time was 12 min for 16 rotators.

IV. Evaluation of the Shuttlecock Optical Rotator

A. Visualization of the Microflow

During the evaluation, the microflows generated by the optical rotators were analyzed. Fig. 10 shows an experimental setup to trap and rotate microobjects with an upward-directed YAG laser beam and to visualize the microflow with different angle illuminations using a high-speed camera. The rotator in the medium inside the coverslip chamber was stably held at the focal point of the $NA = 1.4$ objective lens. Arbitrary-shaped glass particles (density: 2.54 g/m^3, index of refraction: 1.51) ranging from 5 to 15 μm, and the photoresist shuttlecock rotators (density: 1.16 g/m^3, index of refraction: 1.5) of 10 to

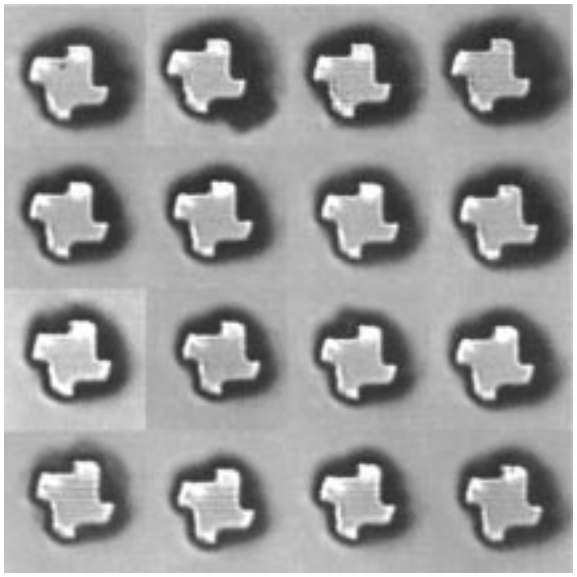

Fig. 9. Shuttlecock optical rotators, 30 μm in diameter 15 μm in thickness fabricated by photoforming.

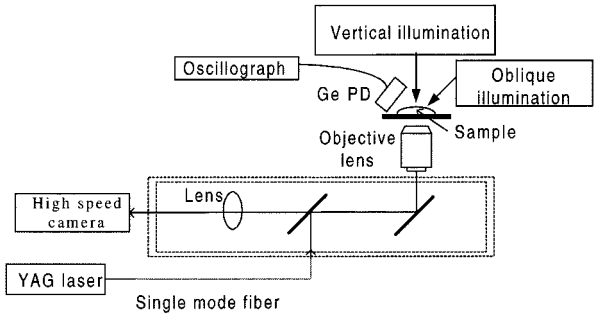

(a)

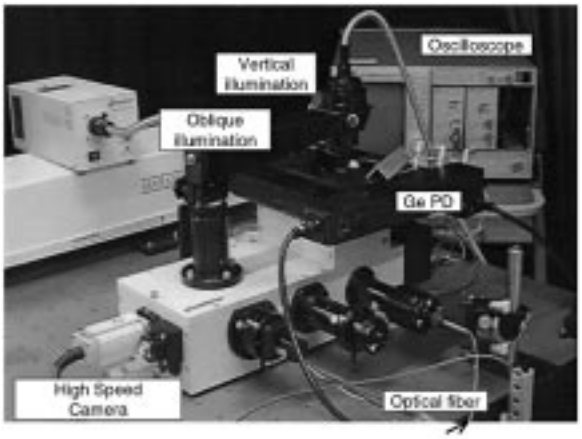

(b)

Fig. 10. Experimental setup to visualize the microflow around the rotator. (a) Block diagram. (b) Photograph. The upward-directed YAG laser traps the rotator and the microflows generated around it are visualized with oblique angle illumination using a high speed camera.

30 μm were used in the experiment. They are transparent to the YAG laser wavelength of 1.06 μm, which avoids optical damage.

In order to visualize the flow field in the proximity of the optical rotator, the following two methods were used. One is the tracer method based on a pathline; various tracers with a diameter of 1 μm were suspended in the glycerol solution and the pathlines were obtained as the tracer movement through successive digital images. The other is the optical method based on medium density variation; various colloids suspended in glycerol solution were illuminated at a grazing angle and the scattered light was observed.

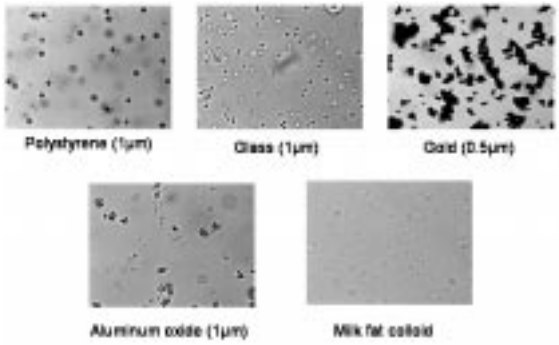

Fig. 11. Trial particles to visualize the microflow.

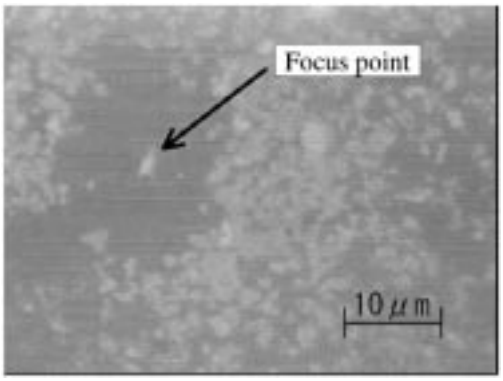

Fig. 12. Effect of the optical pressure. Gold particles around the laser spot are expelled by the optical pressure.

Tracers added to mark the flow included polystyrene, glass, gold, aluminum oxide, diamond, tooth powder, pigment, a shape colloid and a milk fat colloid. Some of them are shown in Fig. 11. The polystyrene and glass are spheres, but the gold and aluminum had no definitive shapes. The particles were dispersed in water with a surface active agent, but the gold and aluminum were condensed due to the electrostatic force.

The requirements for the tracers used with an optical rotator are: 1) their sizes must be small (less than 1 μm in this case) and sufficiently dense; 2) the tracers should be prevented from undergoing Brownian motion; and 3) the tracers should not be affected by optical pressure. Condition 1 is derived from an optical rotator size of about 10 μm, and condition 2 is satisfied by using glycerol to increase the medium viscosity. Since high density glycerol affects the rotator motion, heavy glass beads are adequate for the tracer. Furthermore, particles such as polystyrene, glass, and milk fat colloid were not significantly affected by the optical pressure, but metallic particles such as gold and aluminum oxide were expelled from the laser focal point as shown in Fig. 12.

Table I compares the evaluation results of the visualized images for a number of different kinds of tracer and medium combinations. The symbol ◯ indicates excellent, △ good and ×

TABLE I
THE EFFECT OF THE TRACER ON THE MICRO-FLUIDIC VISUALIZATION

Tracer (Diameter:μm)	Glycerol (%)	Visualization	
		Tracer	Optical
Polystyrene (0.5μm)	50	×	×
Polystyrene (1.0μm)	30	•	×
Glass (0.5μm)	50	×	×
Glass (1.0μm)	30	○	×
Aluminum (1.0μm)	30	×	×
Gold (0.5μm)	50	×	×
Milk fat colloid	30	○	○

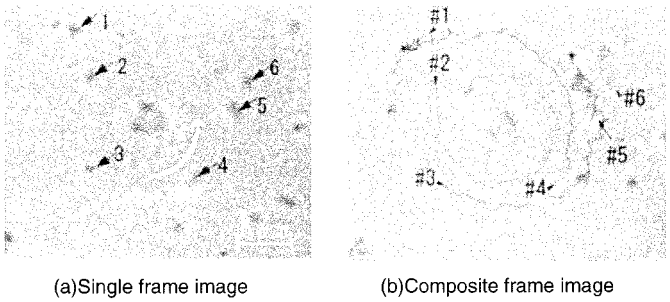

Fig. 13. Visualization and pathlines using glass tracers. (a) Single frame image. (b) Analyzed pathlines.

poor, which suggests that 1 μm diameter glass beads and milk fat colloid are adequate for the microflow visualization.

B. Microflow Analysis

Fig. 13 shows the analyzed results of the microflow. The left figure shows the tracer method for the 1-μm glass beads in 30% glycerol solution. We recorded a 2.3-s motion (71 frames) through a high speed camera. The resolution was 640 × 240 dots × 8 bits per frame. The velocity and the direction of each bead #1 through #6 was traced as the pathlines in the figure. From the figure, the following interesting characteristics of the microflow are recognized: 1) the flows are large for tracers #2, #3, and #4, very close at the rotator but small for #1, #5, and #6, at very distant locations and 2) the flows expand to twice or three times the rotator diameter. Fig. 14 shows the variation in the tracer velocity due to the rotator and the Brownian motion. The microflow and the diffusion effect will promote the stirring or mixing in the microscale systems.

Fig. 15 shows the analyzed velocity vectors around the rotator by the optical method for (a) a broken glass particle and (b) a shuttlecock rotator. The oblique illumination increases the image contrast, because only the scattered light was observed. We can see the microflow around the rotators. We can also recognize the microflow entering at the lower right in the left figure. Compared to the tracer method, this optical method can easily obtain the whole image of the microflow. We will then analyze the microflow by using the visualized images obtained from the optical method.

These flow field analyzes can be done by the fast pattern tracking algorithm based on the correlation between the density variation patterns (Flow-vec32, Library Corp.). Table II summarizes the relationship between the rotation angle, flux amount, and reliability for the broken glass rotator at 56 rpm. The rotation angle per frame is 11.2°. The flux amount is defined here as the total sum of the absolute $\mathbf{v}$ in the visualized images, ranging 50 μm (lateral size) and 38 μm (perpendicular size), where $\mathbf{v}$ is the velocity vector. Reliability means the pattern tracking accuracy for the density variation. From this table, the reliability becomes more than 95% for the analysis between the successive frame but less than 80% for a thinned-out operation. This means that the density variation pattern is kept within one frame (33 ms), but the pattern will be destroyed after two frames which leads to a low correlation (reliability).

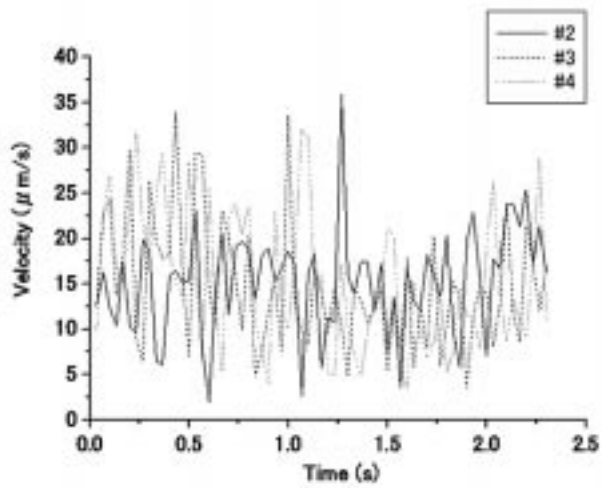

Fig. 14. Variation in the tracer velocity due to the rotator and the Brownian motion.

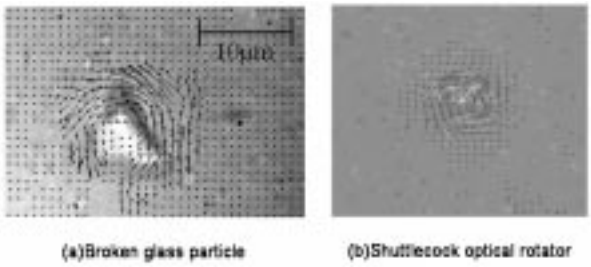

Fig. 15. Visualization and velocity vectors around an optical rotator by milk fat colloid. (a) Broken glass particle. (b) Shuttlecock optical rotator.

TABLE II
RELATIONSHIP BETWEEN FLUX AMOUNT AND RELIABILITY

Tracer (Diameter:μm)	Glycerol (%)	Visualization	
		Tracer	Optical
Polystyrene (0.5μm)	50	×	×
Polystyrene (1.0μm)	30	•	×
Glass (0.5μm)	50	×	×
Glass (1.0μm)	30	○	×
Aluminum (1.0μm)	30	×	×
Gold (0.5μm)	50	×	×
Milk fat colloid	30	○	○

C. Effect of the Rotator Shape and Rotation Rate

Fig. 16 shows the effect of the rotator shape and rotation rate on the flux amount, where the radiation power is 150 mW. The rotation rate is measured by the temporal variation in the scattered light from the rotating particle [19]. The flux amount be-

Particle number	I	II	III	IV
Particle shape				
Rotation speed [rpm]	137	105	60	90
Flux amount [μm/s]	6412	4711	3621	3507

Fig. 16. The effect of the rotator shape on the flux amount, where the radiation power is 150 mW.

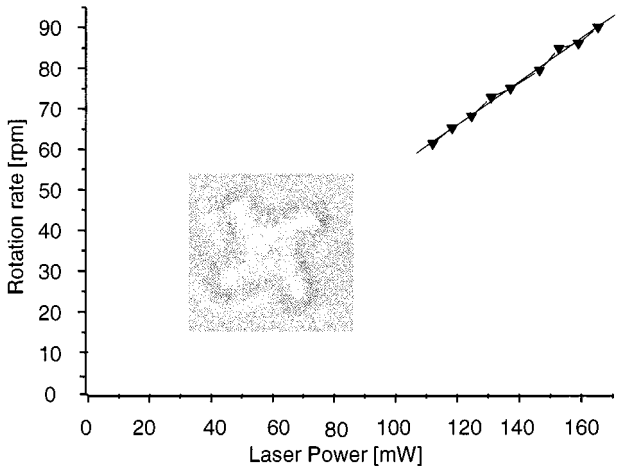

Fig. 17. Relationship between rotation rate and laser power for a shuttlecock optical rotator 10 μm in diameter.

comes larger for rotators #1, #2, and #3 (triangular like shape) compared to rotator #4 (square like shape) because the former rotators contact large liquid area. We also observed that the higher the rotation rate, the larger the flux amount. These results show that both the rotator shape and the rotation rate affect the flux amount.

Fig. 17 shows the relationship between the rotation rate and laser power for a 10 μm diameter shuttlecock optical rotator. The rotation rate is linearly proportional to the laser power. The flux amount generated by the shuttlecock optical rotator is shown in Fig. 18 with the rotation rate as a parameter. We can see that the microflow expands as the rotation rate increases, which corresponds to the result obtained by Fig. 16.

V. Conclusion

In microscale systems, the Reynolds number is so small (less than one), that the flow adopts a laminar profile. In order to promote a convective mixing performance, a shuttlecock optical rotator, which rotates in fluids and is capable of stirring the fluid around it, is proposed and the following basic technologies are confirmed

1) rotator shape design by analyzing the optical torque using a ray optics model,
2) microflow analysis around the rotator using a CFD method,

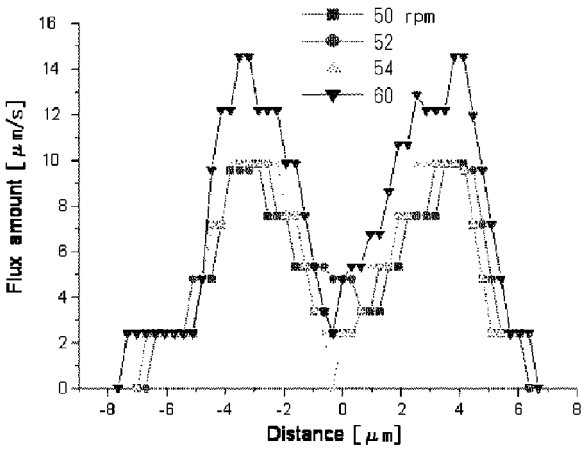

Fig. 18. Flux amount generated by the shuttlecock optical rotator, the rotation rate as a parameter.

3) rotator fabrication both by photolithography using a photoresist and microphotoforming with a visible light-curable resin,
4) flow visualization using milk fat colloid in glycerol solution with grazing angle illumination,
5) pathline and velocity vector analysis close to the rotator, and
6) flow field and flux amount analyzes around the rotator.

It is recognized that the fluidic velocity vector appears within two to three times the rotator diameter in the plane perpendicular to the rotation axes, and the flow goes not only outward, but also upward which promotes the convective mixing performance. The remotely driven, friction-free, and self-aligned characteristics are advantages of the optical pressure rotation. It requires no mechanical connection to a battery and works even in the presence of electromagnetic noise.

These kinds of microliquid stirrings generated by the optical rotator could be of much help in the construction of miniaturized fluidic mix devices in the future.

Acknowledgment

The authors would like to thank Prof. Y. Ogami, Prof. O. Tabata, Prof. S. Konishi of Ritumeikan University for their cooperation, and S. Hiura and K. Yamano of Denken Engineering Co. for the trial manufacture of a microphotoforming apparatus. They would also like to thank graduate students K. Nagatomi, K. Nagumo, S. Tachibana, T. Saitoh, A. Tomimura, M. Idaka, M. Oyoshihara, M. Makita, and T. Inokuchi of Ritumeikan University for their help with the experimental and theoretical analysis and the fabrication of the rotator.

References

[1] A. Ashkin, "History of optical trapping and manipulation of small-neutral particle, atom, and molecules," *IEEE J. Select. Topics Quantum Electron.*, vol. 6, pp. 841–856, June 2000.
[2] M. A. Burns, B. N. Johnson, S. N. Brahmasandra, K. Hndique, J. R. Webster, M. Krishnan, T. S. Sammarco, P. M. Man, D. Jones, D. Heldsinger, C. H. Mastrangelo, and D. T. Burke, "An integrated nanoliter DNA analysis device," *Science*, vol. 282, pp. 484–487, Oct. 1998.

[3] K. P. Kämper *et al.*, "Microfluidic components for biological and chemical microreactors," in *Proc. MEMS*, Nagoya, Japan, Jan. 1997, pp. 338–343.
[4] A. Bertsch, S. Heimgartner, P. Cousseau, and P. Renaud, "3D micromixers-downscaling large scale industrial static mixers," in *Tech. Dig. MEMS*, Interlaken, Switzerland, Jan. 2001, pp. 507–510.
[5] Y. K. Lee, J. Deval, P. Tabeling, and C. M. Ho, "Chaotic mixing in electrokinetically and pressure driven micro flows," in *Technical Digest of the MEMS*, Interlaken, Switzerland, Jan. 2001, pp. 483–486.
[6] P. Woias, K. Hauser, and E. Y. George, "An active silicon micromixer for μ TAS applications," in *Proc. μ TAS*, Enschede, The Netherlands, May 2000, pp. 2277–2282.
[7] J. M. Bustillo *et al.*, "Surface micromachining for microelectromechanical systems," *Proc. IEEE*, vol. 86, pp. 1552–1574, Aug. 1998.
[8] T. Nakamoto, K. Yamaguchi, P. Abraha, and K. Mishima, "Manufacturing of three-dimensional micro-parts by UV laser induced polymerization," *J. Micromech. Microeng.*, vol. 6, pp. 240–253, 1996.
[9] H. Ukita and A. Tomimura, "High resolution micro-photoforming using a spinner laminated layer and a DVD optical head" (in Japanese), *J. Jpn. Soc. Proc. Eng.*, vol. 65, pp. 1360–1364, Sept. 1999.
[10] H. Ukita and M. Idaka, "Visualization and analysis of a micro-flow generated by an optical rotator," *Opt. Rev.*, vol. 7, pp. 448–450, Sept./Oct. 2000.
[11] P. Freymuth, "Flow visualization in fluid mechanics," *Rev. Sci. Instrum.*, vol. 64, pp. 1–18, Jan. 1993.
[12] E. Higurashi, H. Ukita, H. Tanaka, and O. Ohguchi, "Optically induced rotation of micro-objects fabricated by surface micromachinings," *Appl. Phys. Lett.*, vol. 64, pp. 2209–2210, Apr. 1994.
[13] R. C. Gauthier, "Ray optics model and numerical computations for the radiation pressure micro-motor," *Appl. Phys. Lett.*, vol. 67, pp. 2269–2271, Oct. 1995.
[14] K. Nagatomi and H. Ukita, "Improvement in optical rotation rate of a cylindrical micro-objects by incident beam profiles," in *Technical Digest International Conference on Optical MEMS and Their Applications (MOEMS '97)*, Nara, Japan, Aug. 1997, pp. 190–194.
[15] U. D. Larsen, W. Rong, and P. Telleman, "Design of rapid micromixers using CFD," in *Transducers'99*, Sendai, Japan, June 1999, pp. 200–203.
[16] K. Nagumo, Y. Ogami, K. Nagatomi, and H. Ukita, "Investigation on mixing performance by a shuttlecock optical micro-rotor," in *ISROMAC-2000*, Hawaii, Mar. 2000, pp. 452–457.
[17] L. Paterson, M. P. MacDonald, J. Arlt, W. Sibbett, P. E. Bryant, and K. Dholakia, "Controlled rotation of optically trapped microscopic particles," *Science*, vol. 292, pp. 912–914, May. 2001.
[18] S. Maruo, K. Ikuta, and K. Hayato, "Light-driven MEMS made by high-speed two-photon microstereolithography," in *Tech. Dig. MEMS*, Interlaken, Switzerland, Jan. 2001, pp. 594–597.
[19] A. Yamamoto and I. Yamaguchi, "Measurement and control of optically induced rotation of anisotropic shaped particles," *Jpn. J. Appl. Phys.*, vol. 34, pp. 3104–3108, June 1995.

Hiroo Ukita was born in Matsuyama, Japan, on August 28, 1945. He received the Dr.Eng. degree from Tohoku University, Sendai, Japan, in 1973.

He joined Nippon Telegraph and Telephone Corporation in 1973. He has worked in the field of optical disk memory and optical MEMS. Since 1995, he has been with Ritsumeikan University serving as a professor of the faculty of science and engineering. His current interests covers micromechanical photonics which has emerged from the fusion of photonics, mechanics, and electronics, and also optical tweezers which has the possibility of supplying microenergy remotely. He has received 1990 best paper award at the Optical Memory Symposium and also received 1994 Precision Engineering Award from Japan Society for Precision Engineering.

Prof. Ukita is a member of the American Association for the Advancement of Science, the IEEE LEOS Society, the Optical Society of Japan, the Laser Society of Japan, the Japan Society of Applied Physics, the Japan Society for Precision Engineering, the Institute of Electronics, Information and Communication Engineers of Japan. Since 1987, he has worked for the Committee of the International Symposium on Optical Memory and the Microoptics Conference, and currently he serves as a editorial board of the Optical Society of Japan and the Smart Materials and Structures.

Motoki Kanehira received the B.S. degree in optical engineering from Ritsumeikan University in 2000, where he is currently working toward the M.S. degree.

His research interests include an application of optical trapping or optical tweezers.